The Journal of Infectious Diseases

Prostaglandin E2-mediated impairment of innate immune response to A(H1N1)pdm09 infection in diet-induced obese mice could be restored by paracetamol

--Manuscript Draft--

Manuscript Number:	JID-64937R1
Full Title:	Prostaglandin E2-mediated impairment of innate immune response to A(H1N1)pdm09 infection in diet-induced obese mice could be restored by paracetamol
Short Title:	Paracetamol restored innate response
Article Type:	Major Article
Section/Category:	Pathogenesis and Host Response
Keywords:	obesity; immune impairment; influenza; PGE2; paracetamol
Corresponding Author:	Kwok-Yung Yuen The University of Hong Kong Pokfulam, Hong Kong HONG KONG
Corresponding Author Secondary Information:	
Corresponding Author's Institution:	The University of Hong Kong
Corresponding Author's Secondary Institution:	
First Author:	Anna J.X. Zhang
First Author Secondary Information:	
Order of Authors:	Anna J.X. Zhang
	Houshun Zhu
	Yanxia Chen
	Chuangen Li
	Can Li
	Hin Chu
	Leonardi Gozali
	Andrew C.Y. Lee
	Kelvin K.W. To
	Ivan F.N. Hung
	Kwok-Yung Yuen
Order of Authors Secondary Information:	
Manuscript Region of Origin:	HONG KONG
Abstract:	Objective: To investigate why obesity leads to increased severity of influenza infection. Methods: We employed a mouse model with diet-induced obesity (DIO) to study the innate immune responses induced by influenza virus. Results: The lungs of DIO mice were heavily affected by obesity-associated chronic systemic inflammation with a significant increase in inflammatory cytokines/chemokines. Concurrently, lipid immune mediator prostaglandin E2 (PGE2) was also significantly elevated in DIO mice. However, the DIO mice mounted a blunted and delayed upregulation of mRNA and protein concentrations of interferon-β and inflammatory cytokines/chemokines upon A(H1N1)pdm09 virus (H1N1/415742Md) challenge comparing with those of lean mice. PGE2 concentrations were significantly higher in the lungs of DIO mice comparing to that of lean mice post-challenge. Treatment with paracetamol in challenged DIO mice significantly enhanced the

	expression of interferon-α/β and cytokine genes at days 1 and 3 post infection comparing with that of untreated DIO mice. Furthermore, paracetamol treatment alone started 3 days before virus challenge and continued till 6 days post-challenge, ameliorated the severity of a lethal H1N1/415742Md infection in DIO mice with improved survival. Conclusions: Impaired innate response to influenza in DIO mice is associated with elevated PGE2, which could be restored to some degree by paracetamol treatment.

Prostaglandin E2-mediated impairment of innate immune response to A(H1N1)pdm09 infection in diet-induced obese mice could be restored by paracetamol

Anna J.X. Zhang[1-3], Houshun Zhu[4], Yanxia Chen[1], Chuangen Li[1], Can Li[1], Hin Chu[1-3], Leonardi Gozali[1], Andrew C.Y. Lee[1], Kelvin K.W. To[1-3], Ivan F.N. Hung[4], Kwok-Yung Yuen[1-3]*

[1] Department of Microbiology, Li Ka Shing Faculty of Medicine; [2] Research Centre of Infection and Immunology; [3] State Key Laboratory of Emerging Infectious Diseases; [4] Department of Medicine, The University of Hong Kong, Hong Kong, China.

* Correspondence: Kwok-Yung Yuen, Carol Yu Centre for Infection and Division of Infectious Diseases, Department of Microbiology, The University of Hong Kong, Queen Mary Hospital, Pokfulam Road, Hong Kong Special Administrative Region, China (e-mail: kyyuen@hku.hk).

Keywords: obesity, immune impairment, influenza, PGE2, paracetamol

Running title: Paracetamol restored innate response

Word counts: Abstract: 200; main text: 3266 words

Summary of the article: (36 words)

Low-grade chronic inflammatory state in the respiratory tissue of diet-induced obese mice impairs innate immune response to A(H1N1)pdm09 infection. Treatment with paracetamol restores the interferon and cytokine responses which supports that PGE2 contributes to immune impairment.

Abbreviations

DIO, diet-induced obesity; H1N1/415742Md, mouse adapted A/Hong Kong/415742/2009 (H1N1) virus; PGE2, prostaglandin E2; COX1, cyclooxygenase 1; COX2, cyclooxygenase 2; mPGES1, microsomal prostaglandin E synthase-1; mPGES2, microsomal prostaglandin E synthase-2; cPLA2, cytosolic phospholipases A2; cPGES, cytosolic prostaglandin E2 synthase; 15-PGDH 15-hydroxyprostaglandin dehydrogenase

Abstract

Objective: To investigate why obesity leads to increased severity of influenza infection.

Methods: We employed a mouse model with diet-induced obesity (DIO) to study the innate immune responses induced by influenza virus.

Results: The lungs of DIO mice were heavily affected by obesity-associated chronic systemic inflammation with a significant increase in inflammatory cytokines/chemokines. Concurrently, lipid immune mediator prostaglandin E2 (PGE2) was also significantly elevated in DIO mice. However, the DIO mice mounted a blunted and delayed upregulation of mRNA and protein concentrations of interferon-β and inflammatory cytokines/chemokines upon A(H1N1)pdm09 virus (H1N1/415742Md) challenge comparing with those of lean mice. PGE2 concentrations were significantly higher in the lungs of DIO mice comparing to that of lean mice post-challenge. Treatment with paracetamol in challenged DIO mice significantly enhanced the expression of interferon-α/β and cytokine genes at days 1 and 3 post infection comparing with that of untreated DIO mice. Furthermore, paracetamol treatment alone started 3 days before virus challenge and continued till 6 days post-challenge, ameliorated the severity of a lethal H1N1/415742Md infection in DIO mice with improved survival.

Conclusions: Impaired innate response to influenza in DIO mice is associated with elevated PGE2, which could be restored to some degree by paracetamol treatment.

Introduction

Obesity is associated with a wide range of comorbidities, such as type II diabetes mellitus, cardiovascular disease, hypertension and non-alcoholic fatty liver disease [1, 2], as well as immune dysfunction. Epidemiological studies showed that obese individuals are more susceptible to various kinds of infections [3], with higher incidences of hospital acquired infections such as sepsis, pneumonia, and bacteremia [4, 5], as well as increased risks for post-operative surgical wound infections [6, 7], catheter-related infections and bloodstream infections [8].

During the 2009 H1N1 influenza pandemic, obesity was recognized as an independent risk factor for influenza-related morbidity and mortality [9]. Obese individuals are disproportionately represented among influenza-related hospitalizations [10], intensive care unit admission and death [11]. In recent years, health survey studies have linked obesity to an increased susceptibility to community-related respiratory virus infection, including influenza [12-14]. Obese individuals had a higher risk for infection and hospitalization due to seasonal influenza [12] and respiratory syncytial virus [12-14]. While there is abundant clinical information linking impaired respiratory immune defense with obesity, the exact underlying mechanisms are still unclear. Beck et al. demonstrated that the higher morbidity and mortality caused by influenza in diet-induced obese (DIO) mice was due to reduced natural killer cell activity and poor dendritic cell functions [15]. Impaired type I interferon (IFN) production and high

77 cytokine production[16], reduced CD8+ T cell function and impaired generation and
78 function of memory T cells [17, 18] have also been linked with disease severity in
79 influenza infected obese mice. We previously showed that high serum concentrations
80 of adipokine leptin had a detrimental role in A(H1N1)pdm09 influenza infection, and
81 that neutralizing the circulating leptin improved the survival of virus-challenged DIO
82 mice [19].

83 Obesity induces chronic systemic low-grade inflammation [20, 21] due to the activation
84 of immune cells in adipose tissue which produce pro-inflammatory cytokines, such as
85 interleukin (IL)-6, tumor necrosis factor (TNF)-α, and c-reactive protein [21, 22]. This
86 chronic inflammatory state plays a pivotal role in the development of nearly all kinds
87 of chronic diseases associated with obesity, including diabetes, coronary heart diseases
88 and hypertension [21, 23, 24]. Lipid inflammatory mediator prostaglandin E2 (PGE2)
89 has been reported to be elevated in obese individuals and animal models [25, 26]
90 including our own previous study [19]. PGE2 and other forms of prostaglandins (PGs)
91 are powerful lipid mediators that influence the homeostasis of several organs and
92 tissues. PGE2 exerts both immune stimulating and inhibiting effects on immune cells,
93 thus regulating immune function in different contexts [27, 28]. However, the
94 significance of the altered level of PGE2 in host innate immune defense in a diet
95 induced obese state has not been fully understood. In this study, we used a DIO mouse
96 model to investigate how obesity may modulate the innate immune system in response
97 to influenza virus infection.

Methods

Diet-induced obese mice

DIO mice were raised as previously reported [19] from three-week-old female C57BL/6N mice fed with high-fat diet containing 45% Kcal from fat (D12451, Research Diet Inc, New Brunswick, N. J.). Lean control mice were fed normal pellet chew diet.

Virus, virus inoculation and drug treatment

A dose of 2.1×10^2 PFU of mouse-adapted A/Hong Kong/415742/2009 (H1N1) strain (H1N1/415742Md) [29, 30] was used in mouse challenge experiments. At 12 hours, day 1, 2, 3, 4 and 6 post-challenge, lung tissues were collected for virological, immunological and histological analysis. Intraperitoneal celecoxib, 50 mg/kg/day, was given once daily for 3 days [31]. Intraperitoneal paracetamol, 100 mg/kg/day, was given once daily [32] for 3 days before and 6 days after intranasal virus challenge.

Homogenize mouse lung for RNA extraction and ELISA assay

Left lungs were homogenized in 500 µl of RNA extraction buffer for RNA extraction; while right lungs were homogenized in 1 mL of cold minimum essential medium (MEM) for ELISA and plaque assay.

RNA extraction and real-time reverse transcription-polymerase chain reaction

Total RNA from clarified mouse lung homogenates was extracted and reverse-transcribed to cDNA using oligodT primer. Target genes were amplified by real time PCR on the LightCycler 480 system using gene specific primers (Table 1).

Determination of cytokines/chemokines and PGE2

Mouse serum IL-6, TNF-α, leptin PGE2 was assayed by ELISA Cytokines/chemokines in the lung homogenates were assayed by bead-based multiplex assay [33].

Histological examination of infected mouse lungs

Hematoxylin and eosin stained lung tissues were examined microscopically. The degree of bronchiolar epithelial cell death was assessed by a semi-quantitative scoring method as we previously described [34].

Experimental details of the all above methodology are summarized in the Supplementary Materials.

Statistical analysis

All data were analyzed by a Student's t-test using GraphPad Prism 6 for Windows (GraphPad Software, Inc). Mouse survival rates were analyzed by the Kaplan-Meier method and a log rank test. $P < 0.05$ was considered statistically significant.

Results

Significant elevation in inflammatory cytokines/chemokines concentrations in the lungs of DIO mice

After 16 weeks, the mice on high-fat diet gained almost twice the body weight as the lean control mice (Supplementary Figure S1A). The concentrations of serum leptin (Supplementary Figure S1B) and inflammatory cytokine TNF-α and IL-6 (Supplementary Figure S1C) of the high-fat diet mice were significantly higher than those of the control lean mice. These features demonstrated the successful establishment of diet-induced obese mouse model [16, 19]. To investigate if the systemic inflammatory state in DIO mice affects the respiratory system, we detected concentrations of cytokine IL-6, TNF-α, IL-1β, and IL-18, as well as chemokine concentrations of MIP-1α, MIP-1β, MIP-2, MCP-1, MCP-3, IP-10, GM-CSF, and RANTES in lung homogenates. All tested cytokines/chemokines were significantly elevated in the lung of DIO mice versus the control lean mice (Figure 1). These findings confirmed the presence of an inflammatory state in the respiratory system of DIO mice.

Increased concentration of PGE2 in DIO mice is associated with the upregulation of COX2 mRNA

PGE2 is an important inflammatory mediator that is derived from arachidonic acid through the cyclooxygenase (COX1 and COX2) biosynthesis pathway. The concentrations of PGE2 in the serum and lung homogenates were dramatically higher in the DIO mice than the lean mice (Figure 2A). The expression profiles of the genes

that participates in PGE2 metabolism, showed that COX2 mRNA level was significantly upregulated in the lungs of DIO mice (Figure 2B), while COX1 mRNA level was lower than that of lean mice (Figure 2C). In addition, mRNA expression levels of cytosolic phospholipases A2 (cPLA2), terminal prostaglandin E synthases--microsomal prostaglandin E synthase1,2 (mPGES1, mPGES2) and cytosolic prostaglandin E2 synthase (cPGES) were significantly upregulated in DIO mice, but the mRNA of 15-hydroxyprostaglandin dehydrogenase which catalyzes PGE2 degradation was significantly lower than that of the lean mice (Figure 2D). These results indicate that significant alterations in the PGE2 metabolism leading to a high PGE2 level occurred in the lungs of DIO mice.

Previous studies have reported on leptin upregulation of COX2 in an obese state [35, 36]. Therefore we investigated if the inhibition of COX2 activity could reduce PGE2 production in DIO mice. We found that intraperitoneal injection of COX2 inhibitor celecoxib for 3 days significantly reduced PGE2 in the lung homogenates versus that of solvent-treated control (Figure 2E); a milder effect was observed in the lungs of lean mice as concurrent experimental control (Figure 2E). These results suggested that the increased COX2 activity in DIO mice largely accounted for the elevated PGE2, though other factors may also contribute to PGE2 overproduction in DIO mice.

No detectable histopathological changes in unchallenged DIO mice lung tissue despite abnormal inflammatory cell counts in bronchoalveolar lavage fluid (BALF)

We examined whether the elevated concentrations of inflammatory cytokines/chemokines and PGE2 in unchallenged DIO mice lung were accompanied by detectable histological changes. Compared to lean mice, we detected a statistically significant increase in the total cell count in the BALF of DIO mice (Figure 2F). However, in the histological examination, the lung tissue sections of the DIO and lean mice were not visibly different; there was no interstitial or air space immune cell infiltration, and no vascular congestion was observed in either the DIO or lean mice (Figure 2G).

DIO mice mounted delayed and blunted interferon-β and cytokine/chemokine responses to a lethal H1N1/415742Md virus challenge

Groups of DIO and lean mice were inoculated with a 2.1×10^2 PFU of H1N1/415742Md. The levels of mRNA expression and protein secretion of IFN-α/β and inflammatory cytokines in lung homogenates were determined at 12 hours, 1 day, 2 days, 3 days and 4 days post infection (dpi). Real-time RT-PCR assay showed that the IFN-α expression was not elicited in both DIO and lean mice post-challenge (Figure 3A). Induction of IFN-β occurred in both DIO and lean mice from 2 dpi, but the magnitude of IFN-β expression in the DIO mice was significantly lower than that in the lean mice (Figure 3A). The induction of IL-6, TNF-α and IL-1β genes in DIO mice was also significantly weaker than that in the lean mice, whereas there is no induction of IL-10 in DIO mice (Figure 3A).

We also found that IFN-β secretion in DIO mice lung at 1 and 3 dpi was even lower than that of uninfected DIO mice (day 0), but IFN-β increased in lean mice at 1 and 3 dpi (Figure 3B), though not reaching statistical significant difference with that of day 0. Comparing the concentrations before and after infection showed that the fold increment of IFN-β after infection in lean mice were significantly higher than that in DIO mice (Figure 3C). For cytokines and chemokines, although the DIO mice had significantly higher concentrations of lung IL-1β, IL-6 and TNF-α, as well as chemokines MIP1α, MIP1β, MIP2, MCP1, MCP3, and RANTES before infection, the lung concentrations of these cytokine/chemokines were similar in DIO and lean mice 1 and 3 dpi, except for MCP1/3 which was significantly higher at 1 dpi in DIO mice while IL-1β was significantly higher in lean mice at 3 dpi (Supplementary Figure S2). However, the lung cytokine/chemokine concentrations before and after infection showed significantly lower increments in DIO mice post-challenge, whereas that of the lean mice showed significant induction of IL-1β, TNF-α, as well as chemokines MIP1 α, MIP1β, MIP2, MCP1, MCP3, and RANTES (Figure 3D). These data suggested that despite the higher basal level of cytokines/chemokines in DIO mice lung before infection, further innate immune response to influenza virus infection was blunted.

Histological examinations of the lungs at 1 dpi showed mainly vascular congestion in blood vessels and alveolar wall capillaries in DIO and lean mice with no visible bronchiolar epithelial cell death. But at day 3 dpi, DIO mice showed more severe bronchiolar epithelial cell necrosis when compared with lean mice, which was

manifested as cell debris filling the lumens of bronchioles in H&E stained tissue sections (Figure 4A). Semi-quantitative scoring under microscopy showed that the percentages of bronchiolar sections with bronchiolar cell death were significantly higher in DIO mouse lungs (10/48 bronchiolar sections, 20.8%) than that in lean mouse lungs (2/49, 4.08%) (Figure 4B). Immunohistochemical staining of viral nucleoprotein (NP) of the lung tissue showed significantly more bronchiolar epithelial cell were NP positive in DIO mouse lungs than that of lean mice at 3 dpi (Figure S3). At 3 dpi, we did not observe significant perivascular and peribronchiolar immune cell infiltration in DIO mouse lungs (Figure 4A). DIO mice had higher viral load at 1 and 3 dpi compared to lean mice (Figure 4C). These findings suggested that the DIO mice had an impaired control of viral replication in the early stages of infection.

Upregulation of PGE2 after H1N1/415742Md challenge in DIO mice

Our previous study showed high lung concentration of PGE2 in DIO mice before and after H1N1/415742Md infection [19], but how PGE2 affects the innate immune response to influenza infection in DIO mice was not known. To study the changes of the pulmonary PGE2 biosynthesis pathway caused by H1N1/415742Md infection, the mRNA expression of COX1/COX2, cPLA2, cPGES and mPGES1 and mPGES2 was determined. The results showed a rapid upregulation of the COX1 and COX2 gene 12 hours post-challenge and at 3 dpi, which were significantly higher than that of the lean mice (Figure 5A). cPLA2 was upregulated in the DIO mice at 2 and 3 dpi, and cPGEs

were continuously and significantly upregulated in the DIO mice from 12 hours post-challenge until 4 dpi. However, no significant upregulation of mPGES1 and mPGES2 (Figure 5B) was detected.

H1N1/415742Md infection significantly increased PGE2 in the lungs of DIO mice at 1 and 3 dpi, while the serum PGE2 concentration decreased when compared with that of uninfected DIO mice (Figure 5C, left). In lean mice, a mild increase of serum and lung PGE2 concentrations was detected after H1N1/415742Md challenge (Figure 5C, right). Regardless of the trend of changes, the serum and lung PGE2 concentrations in DIO mice were consistently higher than that of the lean mice. These data suggested an alteration of PGE2 response to influenza virus infection in DIO versus that of lean mice.

Paracetamol treatment enhanced innate lung immune response to influenza virus challenge

We investigated if in vivo treatment with COX2 inhibitor could restore the innate immune response to influenza virus infection in DIO mice. Since paracetamol is a commonly used drug with fewer side effects than celecoxib [37], we chose paracetamol for this study. Intraperitoneal paracetamol (100 mg/kg/day) [32] was administered for 3 days before infection and continued until the day of lung tissue sampling (3 dpi). The lung tissue cytokine mRNA expression showed that the paracetamol-treated DIO mice had a significantly higher expression level of IFN-α/β at 3 dpi versus PBS control (Figure 6A). The mRNA expression of IL-1β, TNF-α and IL-10 significantly increased

256 in the paracetamol-treated DIO mice at 1 dpi, and IL-6 expression increased at 3 dpi
257 versus PBS control (Figure 6B). These data suggested that the IFNα/β and cytokine
258 response to influenza virus infection in DIO mice was improved by paracetamol
259 treatment. Lung viral load determined by real-time PCR showed that paracetamol
260 treated DIO mice had reduced viral load versus PBS control at day 1 dpi, but the
261 difference was not statistically significant (Figure 6C).

262 **Paracetamol treatment reduced morbidity and mortality in H1N1/415742Md**
263 **infected DIO mice**

264 We further determined whether the effect of paracetamol on the cytokines extended to
265 the improvement of the outcomes of H1N1/415742Md infection in DIO mice. Groups
266 of DIO or lean mice were treated with paracetamol for 3 days before virus challenge
267 and for 6 days after virus challenge. DIO mice treated with paracetamol had a lower
268 weight loss (Figure 6D) and their survival was significantly better than PBS-treated
269 DIO mice (53.3% vs. 0%, $p<0.01$) (Figure 6E). In the lean mice, although a slightly
270 reduced body weight loss was achieved in the paracetamol treatment group, the survival
271 rate did not significantly improve (33.3% of treated group versus. 21.4% of PBS group).
272 This finding suggested that paracetamol improve the outcome of influenza-infected
273 DIO mice even in the absence of antiviral treatment.

274

275 **Discussion**

Obesity is associated with an increased risk for respiratory viral infections, especially influenza [38], but the underlying mechanisms are not fully understood. In this study, we showed that while the lungs of DIO mice had increased concentrations of inflammatory cytokines/chemokines and PGE2 in the steady state, DIO mice mounted a delayed and blunted upregulation of interferon-β and inflammatory cytokines/chemokines expression against H1N1/415742Md virus challenge. Treatment with paracetamol, a weak inhibitor of prostaglandin synthesis with in vivo effects similar to selective COX-2 inhibitors, significantly increased the IFN-α/β and inflammatory cytokine gene expression in influenza infected DIO mice. Our findings suggested that the chronic inflammation associated with obesity leads to reduced responsiveness to influenza virus infection, with PGE2 playing a significant role.

In an obese state, excessive accumulation of body fat with increased immune cell infiltration and activation in the adipose tissue lead to an over-production of inflammatory cytokines/chemokines resulting in the characteristic low-grade systemic inflammation [20, 21]. This systemic inflammation is critical to the development of nearly all obesity associated chronic diseases including insulin resistance [23], type II diabetes mellitus [24] and coronary artery sclerosis [39]. In this study, we showed that the respiratory system of DIO mice is at an inflammatory state. But the elevated inflammatory mediators in the lung did not provide better immediate protection against influenza virus challenge. Instead, DIO mice showed a higher lung viral load and more severe respiratory epithelial cell death after infection at 3 dpi comparing with lean

297 control mice. Additionally, we observed reduced upregulations of IFN-α/β and
298 cytokines/chemokines in response to virus challenge. These data suggested that the
299 chronic inflammatory state in the lung milieu in the case of obesity gravely
300 compromises the innate responses to virus infection, resulting in insufficient control of
301 the initial viral replication in DIO mice. The impaired type I interferons and
302 proinflammatory cytokines/chemokines production after influenza infection in DIO
303 mice was consistent with the findings reported by Smith et al. who attributed the
304 immune inhibition effects to imbalanced leptin production[16].

305 Our previous study found that leptin contributed to severe disease in A(H1N1)pdm09
306 infected DIO mice [19]. Leptin is one of the adipokines produced by adipocytes. It has
307 multiple functions including activation of immune cells [40], up-regulation of COX2
308 gene and increase of PGE2 [35]. PGE2 is a lipid metabolite of arachidonic acid and
309 produced by the COX cascade, which includes two distinct isoforms of COX, the
310 constitutive COX1 and the inducible COX2, as well as the constitutive and inducible
311 PGE2 synthase enzymes mPGES1, mPGES2 and cPGES. Elevated PGE2
312 concentrations are a hallmark of most inflammatory lesions. The over-production of
313 PGE2 contributes to severe lung damages caused by highly pathogenic influenza virus
314 in non-obese mice which can be reduced with celecoxib [31] and paracetamol treatment
315 [32]. The current study and our previous report showed the PGE2 was basally increased
316 in DIO mice. The basal upregulation of COX2, mPGES1, cPGES gene, downregulation
317 of 15-hydroxyprostaglandin in DIO mice could lead to increased production of PGE2.

318 This increased production of PGE2 by adipose tissue in obesity state was reported to
319 affect lipolysis locally; when entering into the circulation, affects other organs [26].

320 PGE2 has multiple actions in stimulating or suppressing immune responses. The
321 immune suppressive actions of PGE2 include the inhibition of lung macrophage
322 phagocytosis [27] and macrophage apoptosis [41]. Influenza infection-induced PGE2
323 was shown to inhibit type I interferon production in normal C57BL/6 mice [41]. In
324 cases of age-associated chronic inflammation and impaired immune functions, PGE2
325 was related to the reduced anti-viral responses in old age [42]. Our study suggests that
326 the high basal level of PGE2 may play an important part in the impaired cytokine and
327 interferon response in influenza infected DIO mice We showed that pre-treatment
328 with a commonly used non-steroidal anti-inflammatory agent, paracetamol[32, 43, 44],
329 restored IFN-α/β and inflammatory cytokine/chemokine gene response upon
330 H1N1/415742Md challenge and improved survival in DIO mice. However, since the
331 lung viral load in paracetamol treated DIO mice was only insignificantly reduced versus
332 that of control mice, this does not exclude that paracetamol may have other beneficial
333 effects on influenza infected DIO mice. We postulate that in the context of obesity, lung
334 epithelial and resident immune cells chronically exposed to high concentrations of
335 inflammatory mediators especially to high concentrations of PGE2 may impact on
336 immune cell function and reduces the responsiveness to an incoming infection. Our
337 study has limitations. Crocker JF et al once reported that combination of paracetamol
338 with surfactant Toximul MP8 in neonatal mice with influenza B virus infection caused

higher mortality [45]. So, the actions of paracetamol in different context warrant further investigations. We did not investigate the roles of each inflammatory cytokine/chemokine on respiratory innate defense function in obesity. The application of other non-steroid anti-inflammatory drugs in obese mice models should also be investigated to determine their differential effects in host immune function against virus infection.

Acknowledgement

This work was supported by the Health and Medical Research Fund (Ref no. 15140722) of the Food and Health Bureau, Hong Kong Special Administrative Region Government; It was also partly supported by the donations of the Shaw Foundation Hong Kong, Richard Yu and Carol Yu, Michael Seak-Kan Tong, Respiratory Viral Research Foundation Limited, Hui Ming, Hui Hoy and Chow Sin Lan Charity Fund Limited, and Chan Yin Chuen Memorial Charitable Foundation.

We thank Ms. Winger W.N. Mak for providing valuable technical support. We are grateful to the staff at the Department of Microbiology, Animal Unit of HKU for facilitation of the study. We would like to thank Editage (www.editage.com) for English language editing.

Disclosure

The authors declare that the research was conducted in the absence of any commercial or financial relationships that could be construed as a potential conflict of interest.

References

1. Chandler M, Cunningham S, Lund EM, et al. Obesity and Associated Comorbidities in People and Companion Animals: A One Health Perspective. J Comp Pathol **2017**; 156:296-309.

2. Guh DP, Zhang W, Bansback N, Amarsi Z, Birmingham CL, Anis AH. The incidence of co-morbidities related to obesity and overweight: a systematic review and meta-analysis. Bmc Public Health **2009**; 9:88.

3. Milner JJ, Beck MA. The impact of obesity on the immune response to infection. Proc Nutr Soc **2012**; 71:298-306.

4. Dobner J, Kaser S. Body mass index and the risk of infection - from underweight to obesity. Clin Microbiol Infect **2018**; 24:24-8.

5. Koh GCKW, Peacock SJ, van der Poll T, Wiersinga WJ. The impact of diabetes on the pathogenesis of sepsis. Eur J Clin Microbiol **2012**; 31:379-88.

6. Winfield RD, Reese S, Bochicchio K, Mazuski JE, Bochicchio GV. Obesity and the Risk for Surgical Site Infection in Abdominal Surgery. Am Surgeon **2016**; 82:331-6.

7. Wick EC, Hirose K, Shore AD, et al. Surgical Site Infections and Cost in Obese Patients Undergoing Colorectal Surgery. Arch Surg-Chicago **2011**; 146:1068-72.

8. Dossett LA, Dageforde LA, Swenson BR, et al. Obesity and site-specific nosocomial infection risk in the

intensive care unit. Surg Infect (Larchmt) **2009**; 10:137-42.

9. Louie JK, Acosta M, Samuel MC, et al. A Novel Risk Factor for a Novel Virus: Obesity and 2009 Pandemic Influenza A (H1N1). Clin Infect Dis **2011**; 52:301-12.

10. Jain S, Kamimoto L, Bramley AM, et al. Hospitalized Patients with 2009 H1N1 Influenza in the United States, April-June 2009. New Engl J Med **2009**; 361:1935-44.

11. Fezeu L, Julia C, Henegar A, et al. Obesity is associated with higher risk of intensive care unit admission and death in influenza A (H1N1) patients: a systematic review and meta-analysis. Obes Rev **2011**; 12:653-9.

12. Kwong JC, Campitelli MA, Rosella LC. Obesity and Respiratory Hospitalizations During Influenza Seasons in Ontario, Canada: A Cohort Study. Clin Infect Dis **2011**; 53:413-21.

13. Akiyama N, Segawa T, Ida H, et al. Bimodal effects of obesity ratio on disease duration of respiratory syncytial virus infection in children. Allergol Int **2011**; 60:305-8.

14. Maccioni L, Weber S, Elgizouli M, et al. Obesity and risk of respiratory tract infections: results of an infection-diary based cohort study. Bmc Public Health **2018**; 18.

15. Smith AG, Sheridan PA, Tseng RJ, Sheridan JF, Beck MA. Selective impairment in dendritic cell function and altered antigen-specific CD8+ T-cell responses in diet-induced obese mice infected with influenza virus. Immunology **2009**; 126:268-79.

16. Smith AG, Sheridan PA, Harp JB, Beck MA. Diet-induced obese mice have increased mortality and altered immune responses when infected with influenza virus. J Nutr **2007**; 137:1236-43.

17. Karlsson EA, Sheridan PA, Beck MA. Diet-induced obesity impairs the T cell memory response to influenza virus infection. J Immunol **2010**; 184:3127-33.

399 18. Karlsson EA, Sheridan PA, Beck MA. Diet-induced obesity in mice reduces the maintenance of
400 influenza-specific CD8+ memory T cells. J Nutr **2010**; 140:1691-7.
401 19. Zhang AJ, To KK, Li C, et al. Leptin mediates the pathogenesis of severe 2009 pandemic influenza
402 A(H1N1) infection associated with cytokine dysregulation in mice with diet-induced obesity. J Infect Dis
403 **2013**; 207:1270-80.
404 20. Medzhitov R. Origin and physiological roles of inflammation. Nature **2008**; 454:428-35.
405 21. Monteiro R, Azevedo I. Chronic inflammation in obesity and the metabolic syndrome. Mediators
406 Inflamm **2010**; 2010.
407 22. Fenton JI, Nunez NP, Yakar S, Perkins SN, Hord NG, Hursting SD. Diet-induced adiposity alters the
408 serum profile of inflammation in C57BL/6N mice as measured by antibody array. Diabetes Obes Metab
409 **2009**; 11:343-54.
410 23. Heilbronn LK, Campbell LV. Adipose tissue macrophages, low grade inflammation and insulin
411 resistance in human obesity. Curr Pharm Design **2008**; 14:1225-30.
412 24. Oliver E, McGillicuddy F, Phillips C, Toomey S, Roche HM. Postgraduate Symposium The role of
413 inflammation and macrophage accumulation in the development of obesity-induced type 2 diabetes
414 mellitus and the possible therapeutic effects of long-chain n-3 PUFA. P Nutr Soc **2010**; 69:232-43.
415 25. Hu X, Cifarelli V, Sun S, Kuda O, Abumrad NA, Su X. Major role of adipocyte prostaglandin E2 in
416 lipolysis-induced macrophage recruitment. J Lipid Res **2016**; 57:663-73.
417 26. Garcia-Alonso V, Titos E, Alcaraz-Quiles J, et al. Prostaglandin E2 Exerts Multiple Regulatory Actions
418 on Human Obese Adipose Tissue Remodeling, Inflammation, Adaptive Thermogenesis and Lipolysis.
419 PLoS One **2016**; 11:e0153751.

27. Aronoff DM, Canetti C, Peters-Golden M. Prostaglandin E2 inhibits alveolar macrophage phagocytosis through an E-prostanoid 2 receptor-mediated increase in intracellular cyclic AMP. J Immunol **2004**; 173:559-65.

28. Kalinski P. Regulation of immune responses by prostaglandin E2. J Immunol **2012**; 188:21-8.

29. Zheng B, Chan KH, Zhang AJ, et al. D225G mutation in hemagglutinin of pandemic influenza H1N1 (2009) virus enhances virulence in mice. Exp Biol Med (Maywood) **2010**; 235:981-8.

30. Zhang AJX, Li C, To KKW, et al. Toll-Like Receptor 7 Agonist Imiquimod in Combination with Influenza Vaccine Expedites and Augments Humoral Immune Responses against Influenza A(H1N1) pdm09 Virus Infection in BALB/c Mice. Clin Vaccine Immunol **2014**; 21:570-9.

31. Zheng BJ, Chan KW, Lin YP, et al. Delayed antiviral plus immunomodulator treatment still reduces mortality in mice infected by high inoculum of influenza A/H5N1 virus. Proc Natl Acad Sci U S A **2008**; 105:8091-6.

32. Lauder SN, Taylor PR, Clark SR, et al. Paracetamol reduces influenza-induced immunopathology in a mouse model of infection without compromising virus clearance or the generation of protective immunity. Thorax **2011**; 66:368-74.

33. Lee ACY, To KKW, Zhang AJX, et al. Triple combination of FDA-approved drugs including flufenamic acid, clarithromycin and zanamivir improves survival of severe influenza in mice. Arch Virol **2018**.

34. Li C, Li CG, Zhang AJX, et al. Avian Influenza A H7N9 Virus Induces Severe Pneumonia in Mice without Prior Adaptation and Responds to a Combination of Zanamivir and COX-2 Inhibitor. Plos One **2014**; 9.

35. Vuolteenaho K, Koskinen A, Kukkonen M, et al. Leptin enhances synthesis of proinflammatory mediators in human osteoarthritic cartilage--mediator role of NO in leptin-induced PGE2, IL-6, and IL-8

441 production. Mediators Inflamm **2009**; 2009:345838.

442 36. Gao JC, Tian JX, Lv YY, et al. Leptin induces functional activation of cyclooxygenase-2 through
443 JAK2/STAT3, MAPK/ERK, and PI3K/AKT pathways in human endometrial cancer cells. Cancer Sci **2009**;
444 100:389-95.

445 37. Yelland MJ, Nikles CJ, McNairn N, Del Mar CB, Schluter PJ, Brown RM. Celecoxib compared with
446 sustained-release paracetamol for osteoarthritis: a series of n-of-1 trials. Rheumatology **2007**; 46:135-
447 40.

448 38. Mancuso P. Obesity and lung inflammation. J Appl Physiol **2010**; 108:722-8.

449 39. Danesh J, Whincup P, Walker M, et al. Low grade inflammation and coronary heart disease:
450 prospective study and updated meta-analyses. Brit Med J **2000**; 321:199-204.

451 40. Hsieh PS, Jin JS, Chiang CF, Chan PC, Chen CH, Shih KC. COX-2-mediated Inflammation in Fat Is Crucial
452 for Obesity-linked Insulin Resistance and Fatty Liver. Obesity **2009**; 17:1150-7.

453 41. Coulombe F, Jaworska J, Verway M, et al. Targeted prostaglandin E2 inhibition enhances antiviral
454 immunity through induction of type I interferon and apoptosis in macrophages. Immunity **2014**; 40:554-
455 68.

456 42. Elisia I, Lam V, Hofs E, et al. Effect of age on chronic inflammation and responsiveness to bacterial
457 and viral challenges. PLoS One **2017**; 12:e0188881.

458 43. Hinz B, Cheremina O, Brune K. Acetaminophen (paracetamol) is a selective cyclooxygenase-2
459 inhibitor in man. Faseb J **2008**; 22:383-90.

460 44. Sharma CV, Mehta V. Paracetamol: mechanisms and updates. Continuing Education in Anaesthesia
461 Critical Care & Pain **2014**; 14:153-8.

45. Crocker JFS, Digout SC, Lee SH, et al. Effects of antipyretics on mortality due to influenza B virus in a mouse model of Reye's syndrome. Clin Invest Med **1998**; 21:192-202.

Figure legends

Figure 1. Increased concentrations of inflammatory cytokines/chemokines in the lung homogenate of DIO mice. The right lungs collected from DIO mice and control lean mice were homogenized in 1 mL of MEM, clarified supernatant was tested for cytokines/chemokines using bead-based ProcartaPlex Mouse Th1/Th2 & Chemokine Panel 20 Plex Kit. TNF-α was determined by ELISA due to the low sensitivity of the above multiplex kit. The data shown represent the mean value of the two independent experiments from two batches of DIO and lean mice. N=10 for each group. *p<0.05, **p<0.01, ***p<0.001, error bars indicate standard deviations.

Figure 2. Increased PGE2 concentrations and the altered mRNA expression profile of PGE2 biosynthesis-related genes. **A.** Increased concentrations of PGE2 in DIO mice lung and serum, as determined by ELISA assay. Data represent the mean value of two independent experiments from two batches of DIO and lean mice. N=10 for each group. *p<0.05, error bars indicate standard deviations. B-D. Real-time RT-PCR determined mRNA expression level for COX2 (**B**) COX1 (**C**) and other genes as indicated (**D**). The relative expression levels were expressed as 2^-ΔCT. Data presented are mean+SEM. N=10. *p<0.05. **E**. Celecoxib treatment reduced PGE2 concentrations in DIO mouse

lung homogenates. Groups of DIO and lean mice were treated with celecoxib (50 mg/kg/day, once daily, intraperitoneally) for three days, and then sacrificed. PGE2 concentration in the lung homogenates were determined by ELISA assay. Data presented are mean+SEM of two independent experiments. N=6. *p<0.05). F. Increased cellularity in the bronchoalveolar lavage fluid of DIO mice. N=12 each group. *p<0.05. G. No detectable morphological changes in the lung tissue of DIO and lean mice. Representative images of H&E stained lung tissue section. Original magnification 100×.

Figure 3. Reduced IFNα/β and inflammatory cytokines/chemokines induction in DIO mice lungs after A(H1N1)pdm09 virus challenge. Groups of DIO and lean mice were inoculated intranasally with a 2.1×10^2 PFU of H1N1/415742Md virus. At 12h, 1, 2, 3, 4 days post challenge, lungs were collected for analysis. The left lungs were homogenized for RNA extraction and real-time RT-PCR and the right lungs for ELISA or beads-based cytokines/chemokines multiplex assay. **A**. The mRNA expression level of IFN-α, IFN-β, IL-6, TNF-α, IL-β, and IL-10 were expressed as fold change relative to the uninfected DIO or lean mice lung. Data presented are mean+SEM of the two independent experiments. N=6. *p<0.05. **B**. IFN-β concentrations in lung homogenates were determined by ELISA assay. **C.** Degree of increment in the IFN-β concentration induced by virus infection relative to that of uninfected mice. D. Degree of increment in the concentrations of individual cytokines/chemokines induced by virus infection relative to that in uninfected mice. Data presented are mean+SEM of two independent experiments. N=6. *p<0.05, ** p<0.01, *** p<0.001.

Figure 4. Increased lung viral load and lung tissue damage in DIO mouse after A(H1N1)pdm09 challenge. Groups of DIO and lean mice were inoculated intranasally with a 2.1×10^2 PFU of H1N1/415742Md virus. At indicated time-points post-challenge, lungs were collected for analysis. **A**. Representative images of H&E-stained lung tissue section at 3 dpi, original magnification 100× and 400×. **B**. Percentages of bronchiole sections with epithelial cell death in right lungs of infected DIO and lean mice at 3 dpi. N=3 right lungs for each group. *p<0.05. **C.** Viral loads in lung homogenates in plaque forming units are determined on MDCK cells. Data presented are mean+SEM of 8-10 samples of three independent experiments. *p<0.05.

Figure 5. Upregulation of mRNA expression of the genes participating in PGE2 biosynthesis in DIO mice lungs after A(H1N1)pdm09 challenge. Left lungs were collected from groups of DIO and lean mice intranasally inoculated with H1N1/415742Md at 12h, 1, 2, 3 and 4 days post-challenge. Real-time RT-PCR determination of the mRNA expression levels of COX1 and COX2 (**A**); cPLA2, cPGEs, mPGES1 and mPGES2 (**B**), Data were expressed as fold changes relative to the levels in uninfected DIO or lean mice lungs. Data presented are mean+SEM of two independent experiments. N=6. *p<0.05. **C**. PGE2 concentrations in lung homogenates and serum samples of uninfected or infected DIO or lean mice were determined by ELISA assay. Data presented are mean of two independent experiments. N=7-10. Error bars indicate standard deviation.

Figure 6. Paracetamol restored H1N1/415742Md-induced IFNα/β and inflammatory cytokines/chemokines mRNA expression in DIO mice lungs. Groups of DIO mice were treated with paracetamol (100 mg/kg/day, intraperitoneally) once daily for three days, or PBS as control, then inoculated intranasally with 2.1×10^2 PFU of H1N1/415742Md. At 1 and 3 dpi., lung homogenates were analyzed for the mRNA expression of IFN-α/β (**A**) and IL-1β, IL-6, TNF-α, and IL10 (**B**) by real-time RT-PCR. The results were expressed as fold changes relative to the levels in uninfected DIO lungs. Data presented are mean+SEM of two independent experiments. N=6. *p<0.05. **C**. Lung viral load in paracetamol treated and PBS treated control DIO mouse lungs determined by real time RT-PCR amplification of viral M gene. N=3 each group. **D**&**E**. Paracetamol reduced the body weight loss and improved the survival of H1N1/451742Md challenged DIO mice. Groups of DIO or lean mice were treated with paracetamol (100 mg/kg/day, intraperitoneally) once daily for three days, or PBS as control. The mice were then inoculated intranasally with 2.1×10^2 PFU of H1N1/415742Md virus, and received the same treatment until 6 dpi. Body weight and survival were monitored daily until 14 dpi. Data presented are from three independent experiments. N=17, error bars indicate standard deviations. ***p<0.001 when paracetamol-treated DIO mice group were compared to the PBS-treated DIO mice group. Percentages are the survival rate of each group.

Figure1

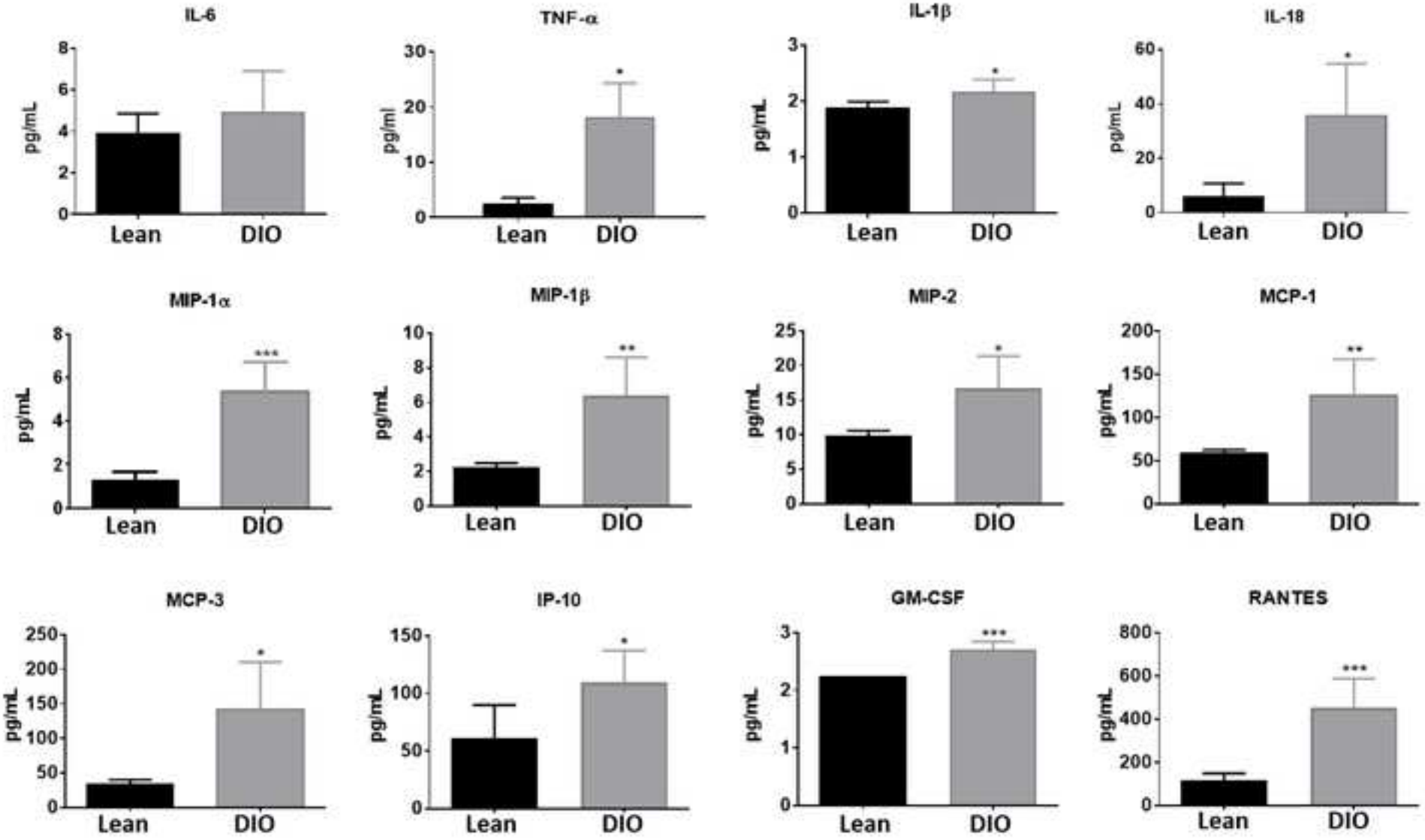

Figure2

Click here to access/download;Figure;AnnaJXZhang-JID-64937-Figure-2-revised.tif

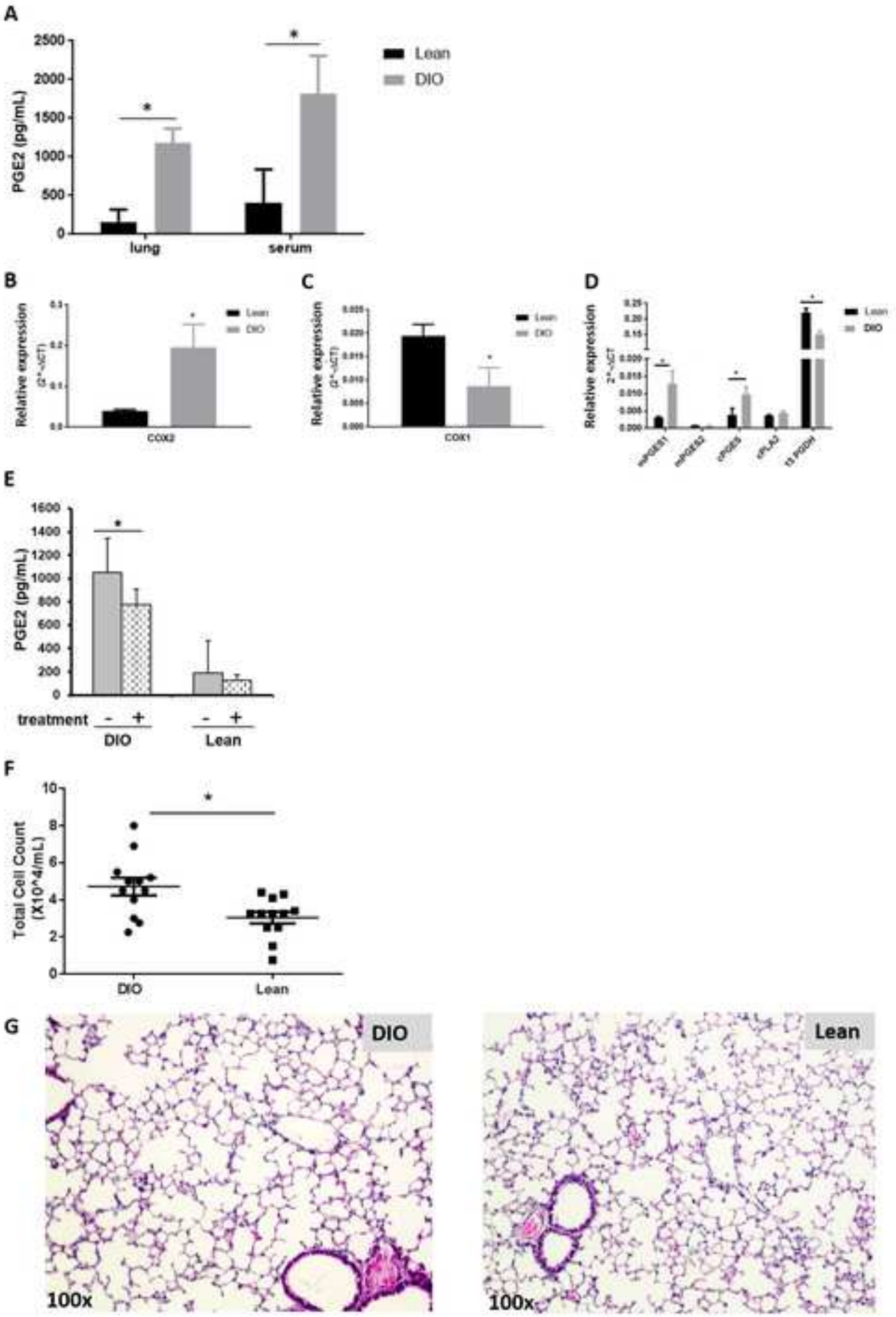

Figure3

Click here to access/download;Figure;AnnaJXZhang-JID-64937-Figure-3-revised.tif

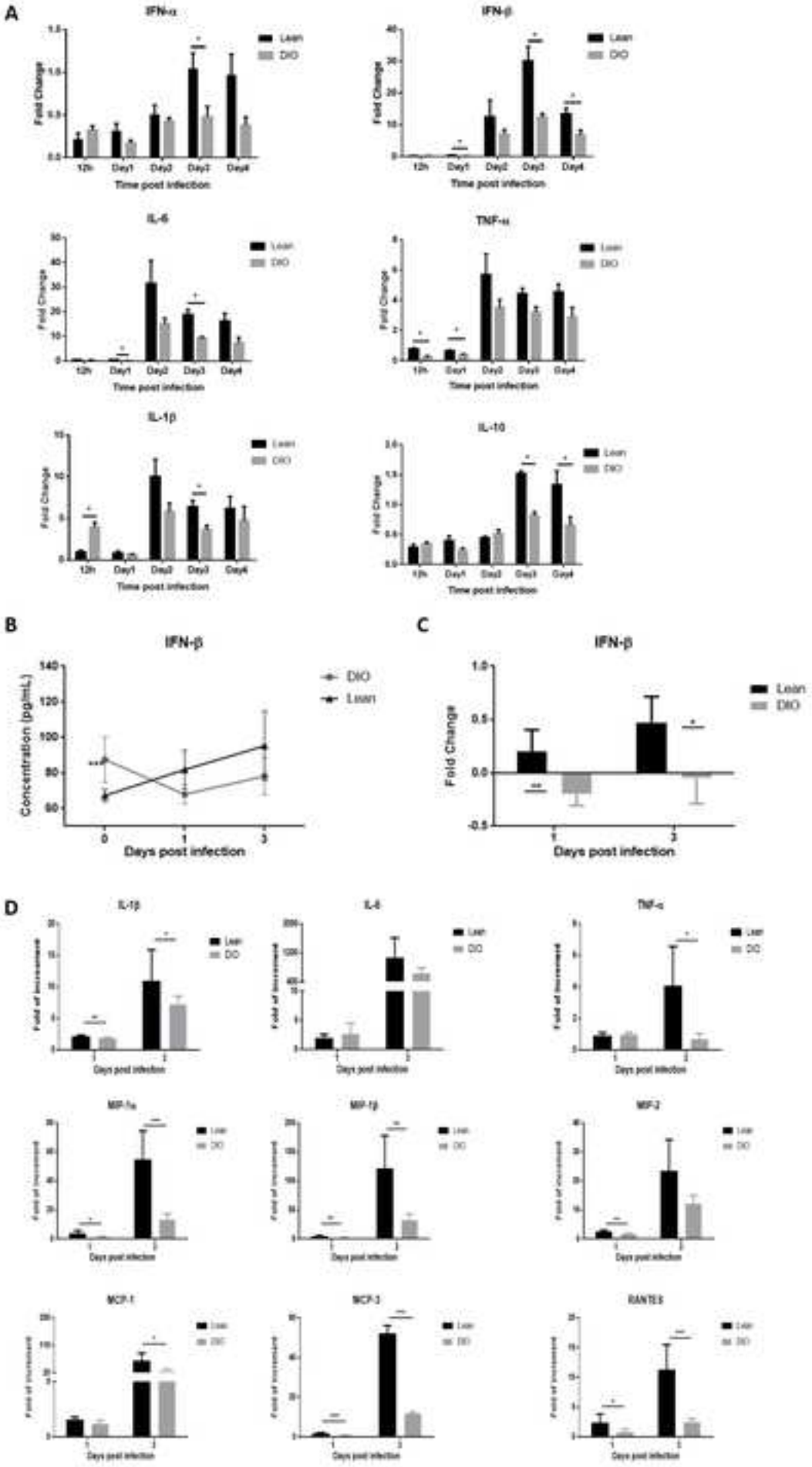

Figure4

Click here to access/download;Figure;AnnaJXZhang-JID-64937-Figure-4-revised.tif

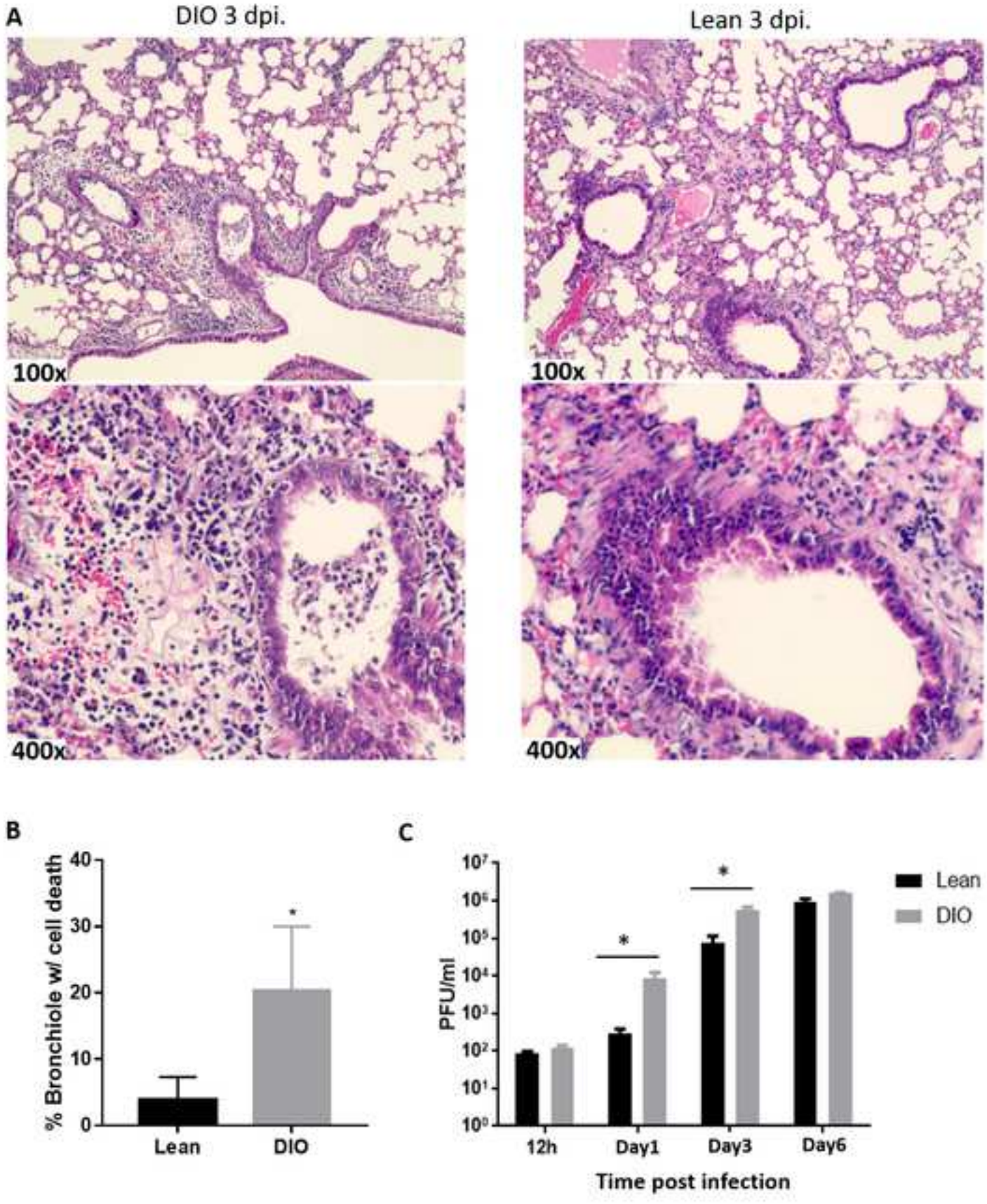

Figure5

Click here to access/download;Figure;AnnaJXZhang-JID-64937-Figure-5-revised.tif

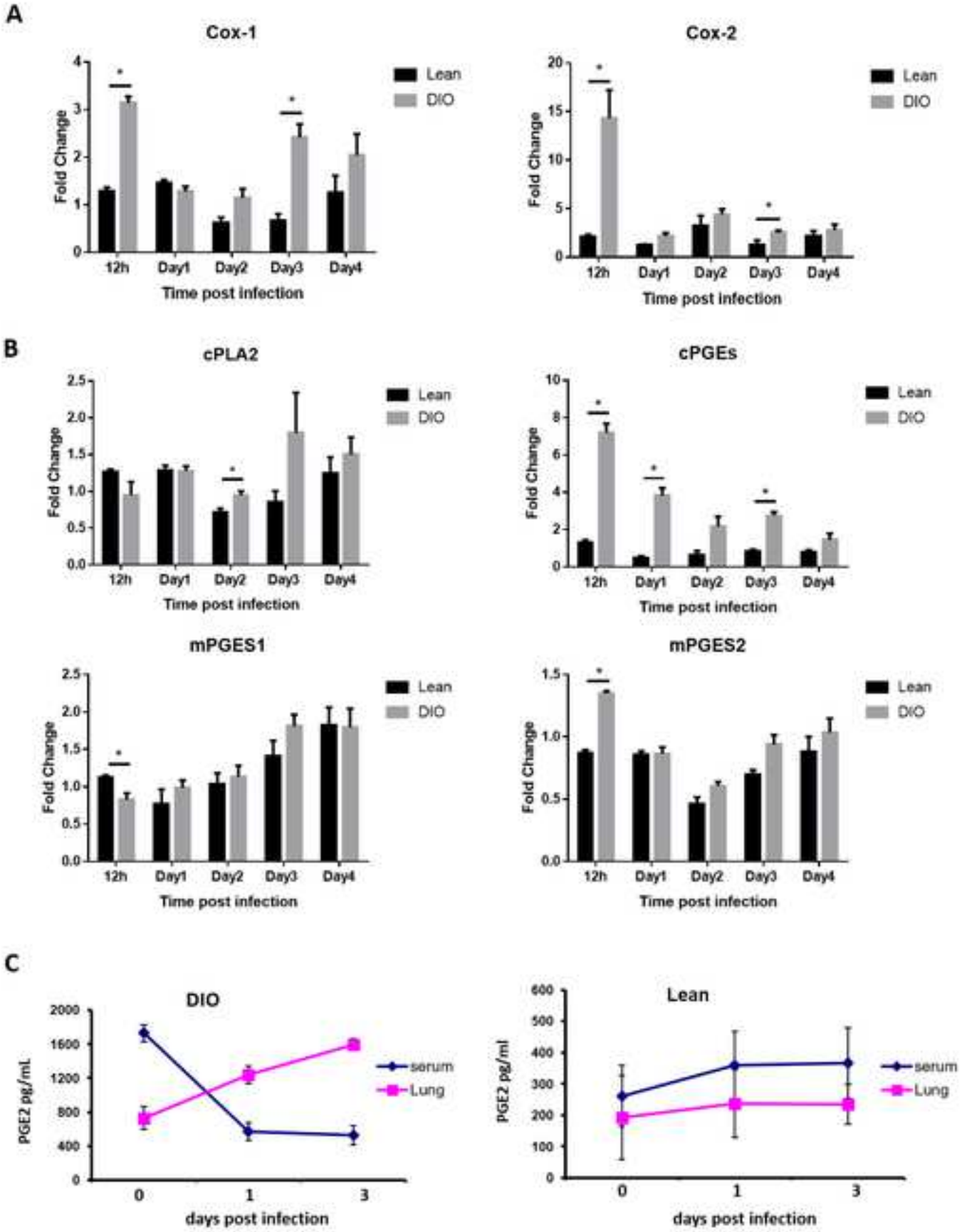

Figure6

Click here to access/download;Figure;AnnaJXZhang-JID-64937-Figure-6-revised.tif

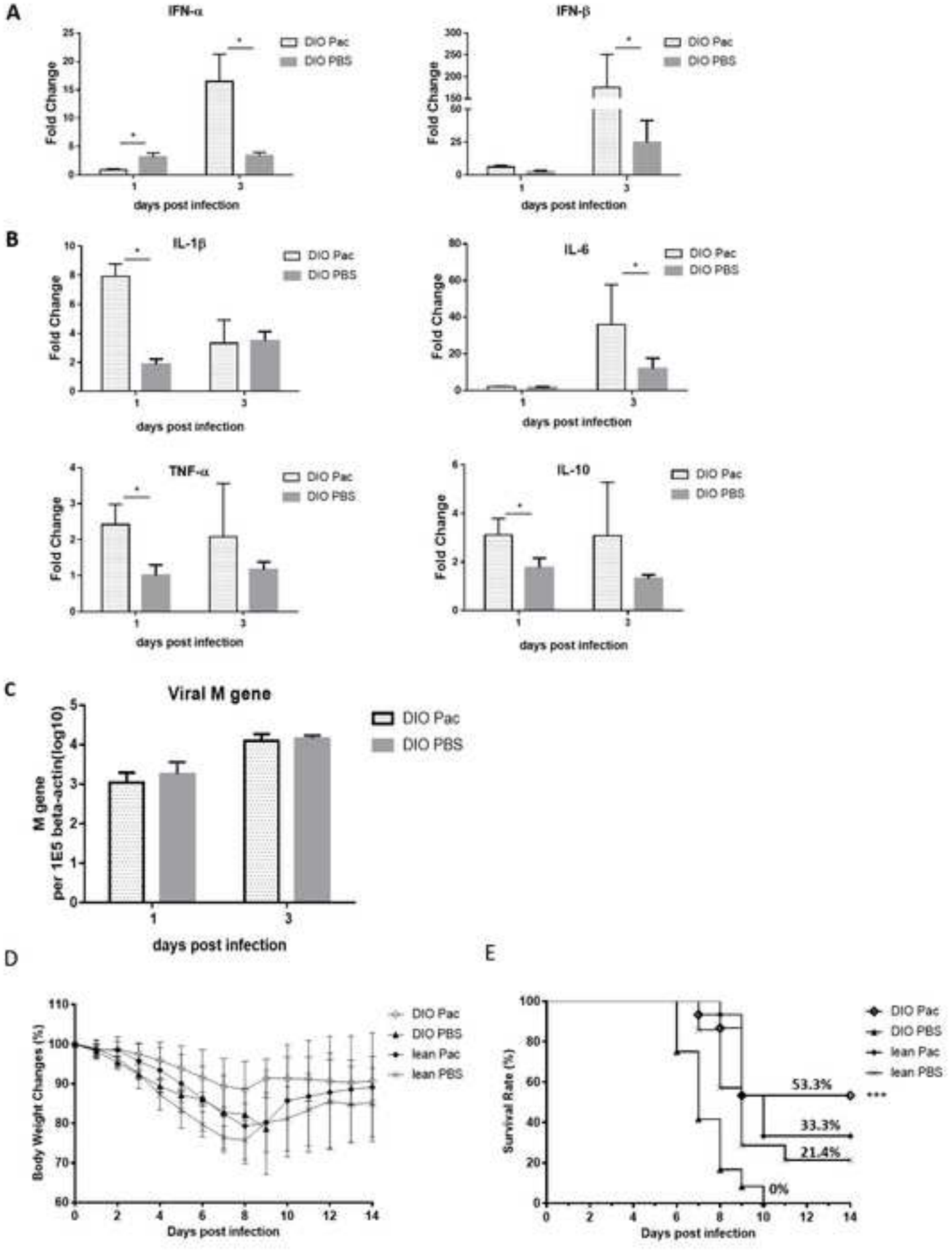

Table 1. Sequences of primers

Gene name	Forward primer (5' to 3')	Reverse Primer (5' to 3')
β-actin	ACGGCCAGGTCATCACTATTG	CAAGAAGGAAGGCTGGAAAAG
IL-6	TGGAGTCACAGAAGGAGTGGCTAAG	TCTGACCACAGTGAGGAATGTCCAC
TNF-α	ATAGCTCCCAGAAAAGCAAGC	CACCCCGAAGTTCAGTAGACA
IL-1β	GCCTTGGGCCTCAAAGGAAAGAATC	GGAAGACACAGATTCCATGGTGAAG
IL-10	CCCTTTGCTATGGTGTCCTT	TGGTTTCTCTTCCCAAGACC
IFN-α	ARSYTGTSTGATGCARCAGGT	GGWACACAGTGATCCTGTGG
IFN-β	TGGGAGATGTCCTCAACTGC	CCTGCAACCACCACTCATTC
COX1	GGCATTGCACATCCATCCAC	CCAGGTCCAGATCTCAGGGA
COX2	TCTGGAACATTGTGAACAACATC	AAGCTCCTTATTTCCCTTCACAC
mPGES1	CCTAGGCTTCAGCCTCACAC	GAAGGTCGCATCCAGCCTAA
mPGES2	AAGGCCATGAATGACCAGGG	TGTTCGGTACACGTTGGGAG
cPGES	CTTTCCTTCTCTCCCGGGTTG	TCTCCTCGCTCCTCTTAGGC
cPLA2	ACGTGCCACCAAAGTAACCA	CCTGCTGTCAGGGGTTGTAG
15PGDH	GCCAAGGTAGCATTGGTGGAT	CTTCCGAAATGGTCTACAACT
Influenza A		
M gene	CTTCTAACCGAGGTCGAAACG	GGCATTTTGGACAAAKCGTCTA

Table1 track change

Table 1. Sequences of primers

Gene name	Forward primer (5’ to 3’)	Reverse Primer (5’ to 3’)
β-actin	ACGGCCAGGTCATCACTATTG	CAAGAAGGAAGGCTGGAAAAG
IL-6	TGGAGTCACAGAAGGAGTGGCTAAG	TCTGACCACAGTGAGGAATGTCCAC
TNF-α	ATAGCTCCCAGAAAAGCAAGC	CACCCCGAAGTTCAGTAGACA
IL-1β	GCCTTGGGCCTCAAAGGAAAGAATC	GGAAGACACAGATTCCATGGTGAAG
IL-10	CCCTTTGCTATGGTGTCCTT	TGGTTTCTCTTCCCAAGACC
IFN-α	ARSYTGTSTGATGCARCAGGT	GGWACACAGTGATCCTGTGG
IFN-β	TGGGAGATGTCCTCAACTGC	CCTGCAACCACCACTCATTC
COX1	GGCATTGCACATCCATCCAC	CCAGGTCCAGATCTCAGGGA
COX2	TCTGGAACATTGTGAACAACATC	AAGCTCCTTATTTCCCTTCACAC
mPGES1	CCTAGGCTTCAGCCTCACAC	GAAGGTCGCATCCAGCCTAA
mPGES2	AAGGCCATGAATGACCAGGG	TGTTCGGTACACGTTGGGAG
cPGES	CTTTCCTTCTCTCCCGGGTTG	TCTCCTCGCTCCTCTTAGGC
cPLA2	ACGTGCCACCAAAGTAACCA	CCTGCTGTCAGGGGTTGTAG
15PGDH	GCCAAGGTAGCATTGGTGGAT	CTTCCGAAATGGTCTACAACT
Influenza A M gene	CTTCTAACCGAGGTCGAAACG	GGCATTTTGGACAAAKCGTCTA

Formatted Table

Formatted: Line spacing: Double

Formatted: Line spacing: Double, Position: Horizontal: Left, Relative to: Margin, Vertical: 1.56", Relative to: Page, Horizontal: 0.13", Wrap Around

Formatted: Line spacing: Double

Supplementary Figure S1

Click here to access/download;Figure;AnnaJXZhang-JID-64937-Supplementary-Figure-S1.tif

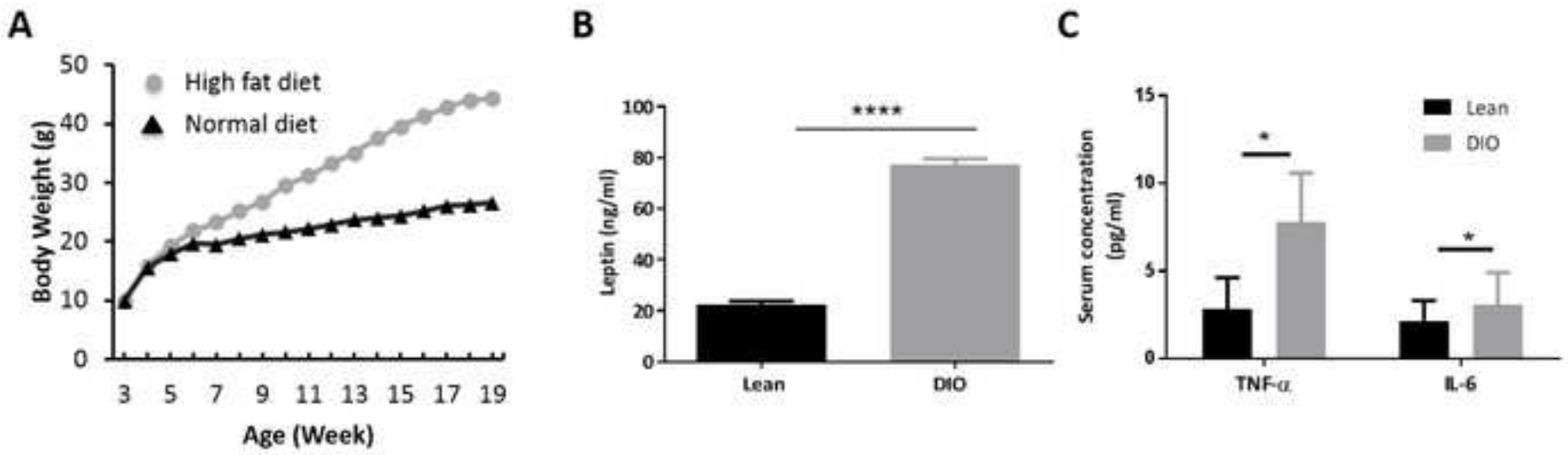

Supplementary Figure S2

Click here to access/download;Figure;AnnaJXZhang-JID-64937-Supplementary-Figure-S2.tif

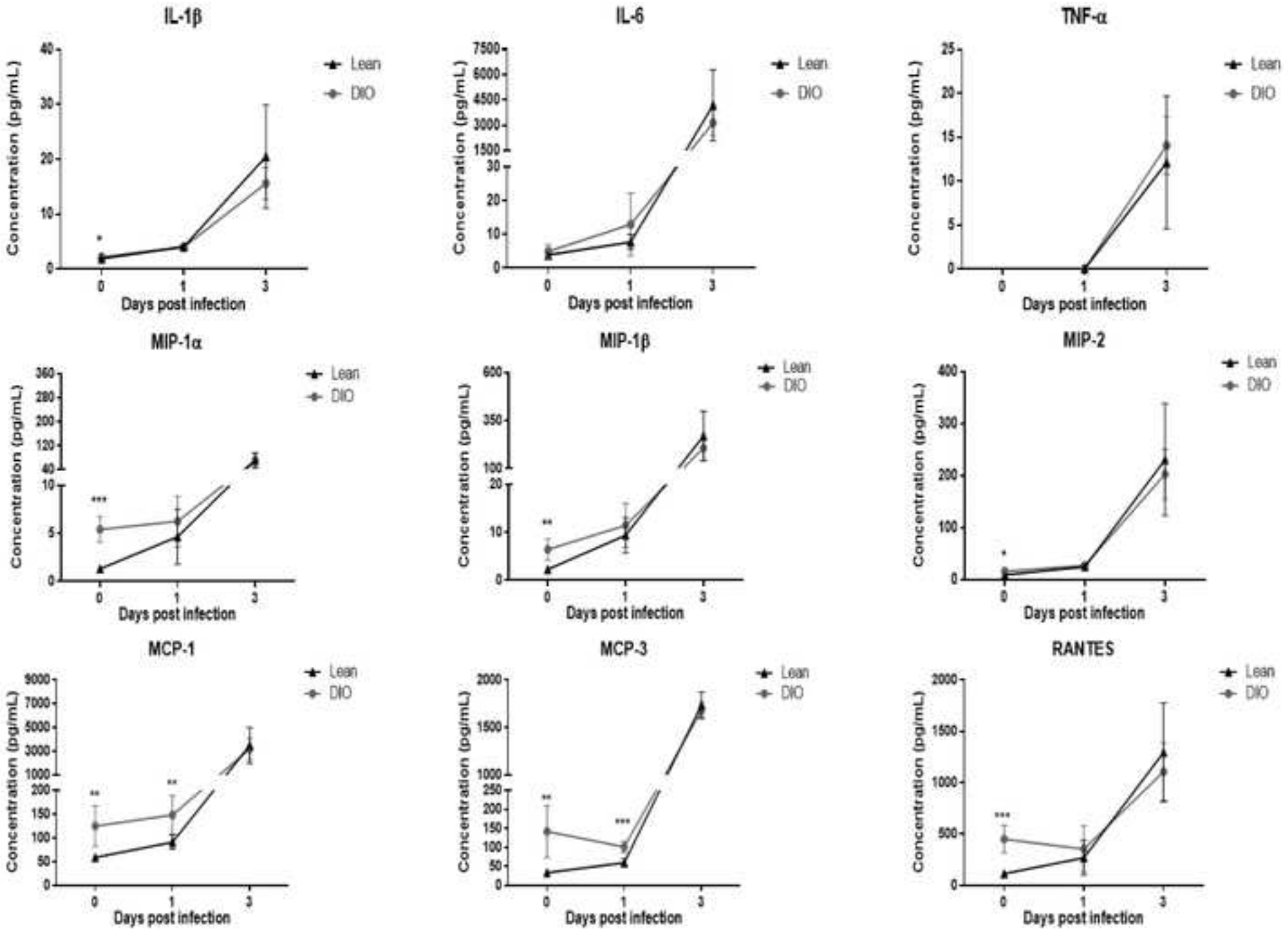

Supplementary Figure S3

Click here to access/download;Figure;AnnaJXZhang-JID-64937-Supplementary-Figure-S3.tif

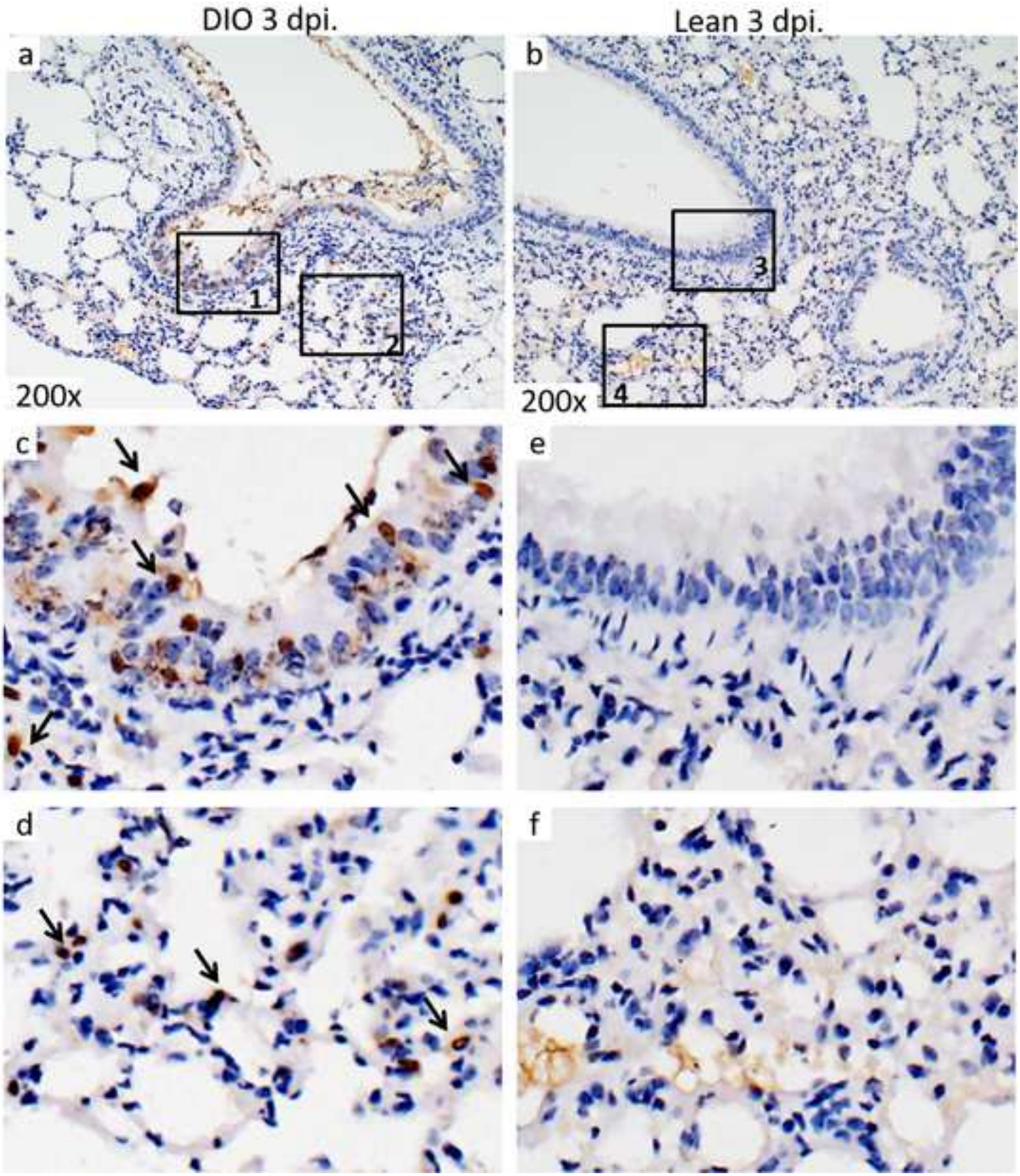

Supplementary figure legend

Figure S1. **A**. Representative body weight chart. Three-week-old female C57BL/6N mice were randomly divided into two groups: one received a high-fat diet and the other, a normal chew diet. The body weights were measured once weekly until 16 weeks on a high-fat diet. The data here showed the average body weight of the mice from three different experiments. Serum concentrations of leptin (**B**), TNF-α and IL-6 (C) measured by ELISA assay after 16 weeks on a high-fat diet. The data represent the mean values of two independent experiments from two batches of DIO and lean mice. Error bars indicate standard deviations. N=10 for each group. *p<0.05, **** p<0.0001

Figure S2. The concentrations of cytokines/chemokines as indicated were determined by bead-based ProcartaPlex Mouse Th1/Th2 & Chemokine Panel 20 Plex Kit. Groups of DIO and lean mice were inoculated intranasally with a 2.1×10^2 PFU of H1N1/415742Md virus. At 1 and 3 dpi, the right lungs were homogenized and clarified supernatant were used for the multiplex assay. Data presented are mean+SEM of two independent experiments. N=6. *p<0.05, **p<0.01, ***p<0.001.

Figure S3. Influenza virus nucleoprotein (NP) detected in mouse lung tissue by immunohistochemical (IHC) staining of paraffin-embedded tissue sections. Representative images of IHC stained DIO lung tissue section (a) and lean mouse lung tissue section (b) at 3 dpi, original magnification 100×. Images showed in c, d, e,

and f were amplified images from areas in square 1, 2, 3, 4, respectively. Arrows indicated NP positive cells stained in brown color.

Supplementary methods

Diet-induced obese (DIO) mice

DIO mice were raised as previously reported [19]. Three-week-old female C57BL/6N mice were randomly divided into two groups: one group was fed a high-fat diet containing 45% Kcal from fat (D12451, Research Diet Inc, New Brunswick, N. J.) while the other was fed a normal pellet chew diet (PicoLab Rodent Diet 20, LabDiet Code 5053, PMI, USA) as control lean mice. All animals were housed under specific-pathogen free conditions with constant room temperature 23±1°C, 12-hour light-dark cycle control and free access to food and water. Their body weights were measured once weekly until the high-fat diet group reached 40-45 gram (about 16-20 weeks on high-fat diet).

Virus, virus inoculation and drug treatment

Mouse-adapted A/Hong Kong/415742/2009 (H1N1) strain, H1N1/415742Md [29, 30] was used in this study. The virus was propagated in 10-day-old SPF chicken embryos at 37°C for 48 hours. Allantoic fluid was harvested and titrated in Madin Darby canine kidney (MDCK) cells for 50% tissue culture infection ($TCID_{50}$) and plaque forming unit (PFU). Aliquots of virus stock were frozen at -80°C until use. Fifty percent mouse lethal dose (LD_{50}) was previously determined to be 2.1×10^2 PFU in 6-8-week-old female BALB/c mice [29, 33]. 2.1×10^2 PFU was used in subsequent mouse challenge experiments.

For virus inoculation, the DIO or lean mice were anesthetized by intraperitoneal injection of ketamine (100 mg/kg) and xylazine (10 mg/kg) diluted in PBS. 2.1×10^{2} PFU of H1N1/415742Md virus in 20 μl was inoculated via intranasal route. Mouse body weight, disease symptoms and survival were monitored daily for 14 days after virus inoculation. At 12 hour, day 1, 2, 3, 4 and 6 after virus challenge, 3-6 mice from each group were sacrificed, and lung tissues were collected for further virological, immunological and histological analysis.

For treatment, celecoxib (Sigma-Aldrich, Steinheim, Germany) was dissolved in dimethyl sulfoxide and further diluted with PBS (final concentration 1% DMSO) for intraperitoneal injection into uninfected mice at 50 mg/kg/day in 200 μl, once daily for 3 days [31], the control group of mice were given same volume of 1%DMSO/PBS injection. Paracetamol (Sigma-Aldrich) dissolved in PBS was also intraperitoneally administered at 100 mg/kg/day once daily [32] for 3 days before and 6 days after H1N1/415742Md infection. The control mice for this treatment were injected with same volume of PBS.

All animal protocols were approved by the Committee on the Use of Live Animals in Teaching and Research, the University of Hong Kong (CULATR ref. 3685-15). Experiments involving live virus were performed in biosafety level 2 animal facilities at the Department of Microbiology, University of Hong Kong.

Homogenize mouse lung tissues for RNA extraction and ELISA assay

At each time point after virus challenge, the mice were euthanized and lungs were taken. Left lungs were homogenized in 500 μl of RNA extraction buffer RLT from

RNeasy Mini kit (Qiagen, Germantown, MD, USA). Homogenates were clarified by centrifugation at 9000×g for 10 min at 4°C.

For the purpose of ELISA and virus titration by plaque assay, right lungs were homogenized in 1 ml of cold minimum essential medium (MEM) supplemented with 1% penicillin and streptomycin. Homogenates were clarified by centrifugation at 9000×g for 10 min at 4°C. The clarified homogenates were aliquoted and stored at -80°C until use.

RNA extraction and real-time reverse transcription-polymerase chain reaction

Total RNA was extracted from 350 µl of clarified homogenates using Qiagen RNeasy Mini kit. 1 µg of total RNA was reverse transcribed into cDNA with oligo-dT primer and PrimeScript^{TM} RT reagent kit (Takara Bio Inc., Shiga, Japan). Each target gene was amplified on LightCycler 480 system (Roche Applied Sciences, Indianapolis, USA) using SYBR Premix Ex Taq II system (Takara Bio Inc., Shiga, Japan) and the gene specific primers listed in Table 1. The expression of house-keeping gene β-actin was analyzed in parallel to normalize the amount of RNA. The ΔΔCt method was applied for the comparison of the differential gene expressions between samples.

The number of viral gene copies in the lung homogenate was determined by quantitative RT-PCR of influenza A M gene with forward primer 5'-CTTCTAACCGAGGTCGAAACG-3'; reverse primer 5'-GGCATTTTGGACAAAKCGTCTA-3', and was expressed as M gene copies per 10^5 copies of β-actin in log scale. The pCR^{TM}II-TOPO vectors containing M gene or β-actin gene were used as standards. The detection limit for influenza A virus M gene in this assay was 100 copies per reaction.

Determination of concentrations of cytokine/chemokine levels and PGE2

Clarified lung homogenate supernatant or serum was assayed according to manufacturers' instructions. Serum IL-6, TNF-α, and leptin were detected using ELISA kits (R&D system, Inc., Minneapolis, MN, USA). The detection limits were 7.8 pg/mL (IL-6,), 10.9 pg/mL (TNF-α) and 62.5 pg/mL (leptin), respectively. PGE2 concentrations in mouse serum and lung homogenate were determined using an ELISA kit from Cayman Chemicals (Ann Arbor, Michigan USA), with detection range of 7.8-1000pg/mL.

The concentrations of cytokines/chemokines in mouse lung homogenate were determined using a beads-based multiplex assay kit (ProcartaPlex Mouse Th1/Th2 & Chemokine Panel 20 Plex Kit, Affymetrix eBioscience, San Diego, CA, USA) according to the manufacture's instruction. Briefly, the Magnetic Capture Beads were added into 96-well plate and washed once with PBS. Individual samples and standards were then added into each well and incubated at room temperature for 2 hours. After three washes, detection antibody mixture was added and allowed to react at room temperature for 30 minutes. After another three washes with PBS and incubated with Streptavidin-PE solution for 30 minutes, the plates were filled with 120 µl Reading Buffer and were read using Luminex xPontent (Luminex, Austin, TX). The data were analyzed using eBioscience ProcartaPlex Analyst 1.0 software. Standard curves were calculated by a five-to-seven-parameter regression formula to fit R2 around 92-99% [33].

Histological examination and semi-quantitative scoring of bronchiolar epithelial cell death in infected mouse lungs

For histological study of mouse lung tissue, additional 3-5 mice were sacrificed at day 1 and 3 post infection. Whole right-side of the lungs were fixed immediately in 10% formalin/PBS, processed and embedded in paraffin blocks. The tissue blocks were cut into 5 μm sections for hematoxylin and eosin (H&E) staining.

H&E stained mouse lung sections were examined by laboratory researchers in blind ways by trained histopathologist. The degree of bronchiolar epithelial cell death was determined by assessing the number of bronchiole sections with dead cell debris in the lumens and bronchiolar epithelial cell necrosis. A semi-quantitative scoring method as described previously [34] was used but with modifications. Briefly, the number of bronchiole in each lung lobe of the whole right lung section was counted under microscope with 40×magnifications. Then, bronchiole cell death was examined under 100× and 200× magnification. The number of bronchiole sections showing cell death was counted, and percentage of which was calculated. Lung histological images were captured with Nikon 80i imaging system with the help of Spot-advance computer software.

Immunohistochemical staining of influenza A nucleoprotein (NP)

Immunohistochemical staining of influenza A nucleoprotein in formalin fixed and paraffin-embedded lung tissue sections was performed as we described in previous report [34]. Briefly, deparaffinized and rehydrated tissue sections were treated with Antigen Unmasking Solution according the manufacturer's instruction (Vector Laboratories Inc. Burlingame, CA, USA) to retrieve antigen. After blocking with 1% bovine serum albumin, the sections were incubated with mouse anti-influenza NP antibody (HB65,

ATCC) at 4ºC for overnight, followed by biotin conjugated goat anti-mouse IgG (Calbiochem, Darmstadt, Germany) for 30 min at room temperature. Streptavidin/ peroxidase complex reagent (Vector Laboratories, Burlingame, CA) was then added and incubated at room temperature for 30 min. Color development was done with 3, 3'-diaminobenzidine (DAB, Vector Laboratories, Burlingame, CA, USA). After counter staining with hematoxylin, the slides were mounted and examined under microscope. Images were captured with Nikon 80i imaging system equipped with Spot-advance computer software.

Lung viral load titration by plaque assay

The clarified lung homogenate supernatants were made 10-fold serial dilutions with Minimum Essential Medium Eagle (MEM) without fetal bovine serum (FBS). Two hundred microliter of diluted samples were inoculated into Madin Darby canine kidney (MDCK) cell monolayer in 12-well plates followed by incubation at 37°C for 1 hour. The cells were then washed with PBS and overlaid with MEM containing 2% low-melting-point agarose and 2 μg/mL of l-1-tosylamide-2-phenylethyl chloromethyl ketone (TPCK). After 72 hours incubation, the cells were fixed in 10% formalin solution and stained with 1% crystal violet. The number of plaque in each well were counted and calculated as plaque forming unit per milliliter.

Collection of cells from bronchoalveolar lavage

This assay was performed in uninfected mice. The mouse was deep anesthetized by intraperitoneal injection of Ketamine/Xylazine. The mouse was placed in the dorsal decubitus position and the trachea was exposed through opening the neck skin with scissors. A small semi-excision was made on the trachea to allow a 21-G lavage tube to pass into the trachea. After stabilizing the tube and needle, 1 mL saline-EDTA was injected into the lung and the fluid was then aspirated. The procedure was repeated 5-6 times per animal to collect as many cells as possible. The cell number was counted with hemocytometer and calculated as total cell count per milliliter.